Effects of isovector scalar δ-meson on hypernuclei

M. Ikram[1], S. K. Singh[2], S. K. Biswal[2] and S. K. Patra[2]
[1] *Department of Physics, Aligarh Muslim University, Aligarh-202002, India*
[2] *Institute of Physics, Sachivalaya Marg, Bhubaneswar-751005, India.*
(Dated: January 16, 2014)

We analyze the effects of $\delta-$ meson on hypernuclei within the frame-work of relativistic mean field theory. The $\delta-$ meson is included into the Lagrangian for hypernuclei. The extra nucleon-meson coupling (g_δ) affects the every piece of physical observables, like binding energy, radii and single particle energy of hypernuclei. The lambda mean field potential is investigated which is consistent with other predictions. Flipping of single particle energy levels are observed with the strength of g_δ in the considered hypernuclei as well as normal nuclei. The spin-orbit potentials are observed for considered hypernuclei and the effect of g_δ on spin-orbit potentials is also analyzed. The calculated single-Λ binding energies (B_Λ) are quite agreeable with the experimental data.

PACS numbers: 21.10.-k, 21.10.Dr, 21.80.+a

arXiv:1401.3608v1 [nucl-th] 15 Jan 2014

I. INTRODUCTION

Normal nuclei are quite informative for showing the distinctive features of nucleon-nucleon (NN) interaction. The knowledge on NN interaction may be extended to hyperon-nucleon (YN) or hyperon-hyperon (YY) interaction by injecting one or more strange baryon to bound nuclear system [1–16]. The injected hyperon originates a new quanta of strangeness and makes a more interesting nuclear system with increasing density [2]. Unlike to nucleons, a hyperon is not Pauli blocked owing to strangeness quantum number and resides at the centre of the nucleus. Hyperons are used as an impurity in nuclear systems to reveal many of the nuclear properties in the dimension of strangeness [17–19]. For this, a slightly unbound normal nucleus can be bound by addition of Λ particle [20, 21].

To understand the structure of strange system, it is necessary to evaluate the contribution of YN interaction. But, due to short life-time of hyperon, only limited information on YN scattering data is available which is a major consequence of the experimental difficulties [22]. For this purpose, more theoretical data are needed to explore the strangeness physics. However, extensive efforts on theoretical basis have been made to enrich the knowledge about YN interaction using relativistic and non-relativistic mean field approaches. For example, Skyrme Hartree-Fock (SHF) [1, 7, 23–25], deformed Hartree-Fock (DHF) [21, 26], Skyrme Hartree-Fock with BCS approach [27] and relativistic mean field (RMF) formalism [3, 4, 20, 28–34].

From last three decades, the relativistic mean field theory reproduces the experimental data on binding energy, root mean square (rms) radius, and quadrupole deformation parameter for finite nuclei throughout the periodic chart [35–42]. Here the degrees of freedom are nucleons and mesons. To deal with hypernuclei, one has to incorporate the meson-hyperon interaction to the relativistic Lagrangian. The most successful RMF model of Boguta and Bodmer, included the $\sigma-$, $\omega-$, and $\rho-$mesons along with the nonlinear coupling of $\sigma-$meson, which simulates the three-body interaction [43]. The $\rho-$meson takes care the neutron-proton asymmetry, while the Coulomb interaction is taken care by the electromagnetic field produced by the protons. Although, conventional RMF model is quite successful, but it is recently realized that the isovector-scalar $\delta-$meson, which arises from the mass and isospin asymmetry of proton and neutron is very important for nuclear system with much difference in neutron N and proton Z number [44–46]. The main objective of the present study is to see the effects of $\delta-$meson for some selected hypernuclear systems. For this purpose, we evaluate the contribution of $\delta-$meson in hypernuclear system and make a comparison with normal nuclei.

The paper is organized as follows: Section II gives a brief description of relativistic mean field formalism for hypernuclei with inclusion of $\delta-$ meson. The results are presented and discussed in Section III. Selection of g_δ and g_ρ coupling constant is also discussed in this section. The paper is summarized in Section IV.

II. FORMALISM

The RMF Lagrangian for hyperon-nucleon-meson many-body system including the $\delta-$ meson is written as [3, 4, 20, 28, 29, 47–49]:

$$\mathcal{L} \;=\; \mathcal{L}_N + \mathcal{L}_\Lambda \;, \tag{1}$$

$$\begin{aligned}
\mathcal{L}_N \;&=\; \bar{\psi}_i\{i\gamma^\mu\partial_\mu - M\}\psi_i + \frac{1}{2}(\partial^\mu\sigma\partial_\mu\sigma - m_\sigma^2\sigma^2) \\
&-\; \frac{1}{3}g_2\sigma^3 - \frac{1}{4}g_3\sigma^4 + \frac{1}{2}(\partial^\mu\delta\partial_\mu\delta - m_\delta^2\delta^2) \\
&-\; g_s\bar{\psi}_i\psi_i\sigma - g_\delta\bar{\psi}_i\vec{\tau}\psi_i\vec{\delta} - \frac{1}{4}\Omega^{\mu\nu}\Omega_{\mu\nu} + \frac{1}{2}m_w^2V^\mu V_\mu \\
&-\; g_w\bar{\psi}_i\gamma^\mu\psi_iV_\mu - \frac{1}{4}B^{\mu\nu}B_{\mu\nu} + \frac{1}{2}m_\rho^2\vec{R}^\mu\vec{R}_\mu \\
&-\; \frac{1}{4}F^{\mu\nu}F_{\mu\nu} - g_\rho\bar{\psi}_i\gamma^\mu\vec{\tau}\psi_i\vec{R}^\mu \\
&-\; e\bar{\psi}_i\gamma^\mu\frac{(1-\tau_{3i})}{2}\psi_iA_\mu \;, \qquad (2) \\
\mathcal{L}_\Lambda \;&=\; \bar{\psi}_\Lambda\{i\gamma^\mu\partial_\mu - m_\Lambda\}\psi_\Lambda - g_{\omega\Lambda}\bar{\psi}_\Lambda\gamma^\mu\psi_\Lambda V_\mu \\
&-\; g_{\sigma\Lambda}\bar{\psi}_\Lambda\psi_\Lambda\sigma \;, \qquad (3)
\end{aligned}$$

where ψ and ψ_Λ denote the Dirac spinors for nucleon and Λ particle, whose masses are M and m_Λ respectively, and $g_{\sigma\Lambda}$, $g_{\omega\Lambda}$ are $\Lambda-$meson coupling constants. Because of zero isospin, the Λ hyperon does not couple to $\rho-$ and $\delta-$mesons. The quantities m_σ, m_ω, m_ρ and m_δ are the masses for $\sigma-$, $\omega-$, $\rho-$ and $\delta-$mesons. The field for the σ-meson is denoted by $\sigma-$, $\omega-$meson by V_μ, $\rho-$meson by R_μ and δ-meson by δ. The quantities g_s, g_ω, g_ρ, g_δ and $e^2/4\pi$=1/137 are the coupling constants for the $\sigma-$, $\omega-$, $\rho-$, $\delta-$mesons and photon, respectively. We have g_2 and g_3 self-interaction coupling constants for $\sigma-$mesons. The field tensors of the vector, isovector mesons and of the electromagnetic field are given by

$$\begin{aligned} \Omega^{\mu\nu} &= \partial^\mu V^\nu - \partial^\nu V^\mu \ , \\ B^{\mu\nu} &= \partial^\mu R^\nu - \partial^\nu R^\mu \ , \\ F^{\mu\nu} &= \partial^\mu A^\nu - \partial^\nu A^\mu \ . \end{aligned} \tag{4}$$

The classical variational principle is used to solve the field equations for bosons and Fermions. The Dirac equation for the nucleon is written as:

$$[-i\alpha.\nabla + V(r) + \beta(M + S(r))]\psi_i = \epsilon_i \psi_i \ , \tag{5}$$

where V(r) and S(r) represent the vector and scalar potential, defined as

$$V(r) = g_\omega V_0(r) + g_\rho \tau_3 \rho_0(r) + e\frac{(1-\tau_3)}{2} A_0(r) \ , \tag{6}$$

and

$$S(r) = g_\sigma \sigma(r) + \tau_3 g_\delta \delta_0(r) \ , \tag{7}$$

where subscript $i =$ n, p for neutron and proton, respectively. The Dirac equation for Λ particle is

$$[-i\alpha.\nabla + \beta\big(m_\Lambda + g_{\sigma\Lambda}\sigma(r)\big) + g_{\omega\Lambda} V_0(r)]\psi_\Lambda = \epsilon_\Lambda \psi_\Lambda \ . \tag{8}$$

The field equations for bosons are

$$\begin{aligned} \{-\triangle + m_\sigma^2\}\sigma(r) &= -g_\sigma \rho_s(r) - g_2\sigma^2(r) - g_3\sigma^3(r) \\ &\quad - g_{\sigma\Lambda}\rho_s^\Lambda(r) \ , \\ \{-\triangle + m_\omega^2\}V_0(r) &= g_\omega \rho_v(r) + g_{\omega\Lambda}\rho_v^\Lambda(r) \ , \\ \{-\triangle + m_\delta^2\}\delta_3(r) &= -g_\delta \rho_3^s(r) \ , \\ \{-\triangle + m_\rho^2\}R_3^0(r) &= g_\rho \rho_3(r) \ , \\ -\triangle A_0(r) &= e\rho_c(r) \ . \end{aligned} \tag{9}$$

Here ρ_s, ρ_s^Λ, ρ_v and ρ_v^Λ are the scalar and vector density for $\sigma-$ and $\omega-$field in nuclear and hypernuclear system which are expressed as

$$\begin{aligned} \rho_s(r) &= \sum_{i=n,p} \bar{\psi}_i(r)\psi_i(r) \ , \\ \rho_s^\Lambda(r) &= \sum \bar{\psi}_\Lambda(r)\psi_\Lambda(r) \ , \\ \rho_v(r) &= \sum_{i=n,p} \psi_i^\dagger(r)\psi_i(r) \ , \\ \rho_v^\Lambda(r) &= \sum \psi_\Lambda^\dagger(r)\psi_\Lambda(r) \ . \end{aligned} \tag{10}$$

The scalar density for $\delta-$ field is

$$\rho_3^s(r) = \sum_{i=n,p} \bar{\psi}_i(r)\tau_{3i}\psi_i(r) \ . \tag{11}$$

The vector density $\rho_3(r)$ for $\rho-$field and charge density $\rho_c(r)$ are expressed by

$$\begin{aligned} \rho_3(r) &= \sum_{i=n,p} \psi_i^\dagger(r)\gamma^0\tau_{3i}\psi_i(r) \ , \\ \rho_c(r) &= \sum_{i=n,p} \psi_i^\dagger(r)\gamma^0\frac{(1-\tau_{3i})}{2}\psi_i(r) \ . \end{aligned} \tag{12}$$

The various rms radii are defined as

$$\begin{aligned} \langle r_p^2\rangle &= \frac{1}{Z}\int r_p^2 d^3r\rho_p \ , \\ \langle r_n^2\rangle &= \frac{1}{N}\int r_n^2 d^3r\rho_n \ , \\ \langle r_m^2\rangle &= \frac{1}{A}\int r_m^2 d^3r\rho \ , \\ \langle r_\Lambda^2\rangle &= \frac{1}{\Lambda}\int r_\Lambda^2 d^3r\rho_\Lambda \ , \end{aligned} \tag{13}$$

for proton, neutron, matter and lambda rms radii respectively and ρ_p, ρ_n, ρ and ρ_Λ are their corresponding densities. The charge rms radius can be found from the proton rms radius using the relation $r_c = \sqrt{r_p^2 + 0.64}$ taking into consideration the finite size of the proton. The total energy of the system is given by

$$\begin{aligned} E_{total} &= E_{part}(N,\Lambda) + E_\sigma + E_\omega + E_\delta + E_\rho \\ &\quad + E_c + E_{pair} + E_{c.m.}, \end{aligned} \tag{14}$$

where $E_{part}(N,\Lambda)$ is the sum of the single particle energies of the nucleons (N) and hyperon (Λ). E_σ, E_ω, E_δ, E_ρ, E_c, E_{pair} and E_{cm} are the contributions of meson fields, Coulomb field, pairing energy and the center-of-mass energy, respectively. We use NL3* parameter set through out the calculations [50].

We adopt the relative $\sigma-$ and $\omega-$ coupling to find the numerical values of $\Lambda-$meson coupling constants. The relative coupling constants for σ and ω field are defined as $R_\sigma = g_{\sigma\Lambda}/g_\sigma$ and $R_\omega = g_{\omega\Lambda}/g_\omega$. We use the value of the relative ω coupling as $R_\omega = 2/3$ from the naive quark model [51, 52]. For used NL3* parameter set, we take the relative σ coupling value as $R_\sigma = 0.620$ [30]. In present calculations, to take care of pairing interaction the constant gap BCS approximation is used and the centre of mass correction is included by the formula $E_{cm} = -(3/4)41A^{-1/3}$.

III. RESULTS AND DISCUSSIONS

The calculated results are shown in Table I and Figs. (1−11) for both normal nuclei and hypernuclei. We study the effect of $\delta-$meson on some selected hypernuclei, like ${}^{48}_{\Lambda}$Ca, ${}^{90}_{\Lambda}$Zr and ${}^{208}_{\Lambda}$Pb. To demonstrate the effect of g_δ on hypernuclei, we make a comparison with their normal nuclear (^{48}Ca, ^{90}Zr and ^{208}Pb) counter parts.

TABLE I: The calculated lambda binding energy, B_Λ for single-Λ hypernuclei is compared with the experimental data [22, 25, 53], given in brackets. The used parameter set is pure NL3* without any inclusion of g_δ. The radii are also displayed. Energies are given in MeV and radii are in fm.

	BE (MeV)	B_Λ(s)	B_Λ(p)	r_c	r_t	r_p	r_n	r_Λ
${}^{16}_{\Lambda}$N	130.04	13.80 (13.76±0.16)	3.56 (2.84±0.16)	2.563	2.468	2.442	2.510	2.302
${}^{16}_{\Lambda}$O	126.44	13.80 (12.5±0.35)	3.56 (2.5±0.5)	2.666	2.476	2.544	2.420	2.301
${}^{28}_{\Lambda}$Si	235.94	20.18 (16.6±0.2)	9.10 (7.0±1.0)	2.991	2.826	2.883	2.800	2.323
${}^{32}_{\Lambda}$S	273.74	21.77 (17.5±0.5)	10.20 (8.1±0.6)	3.158	2.982	3.056	2.943	2.287
${}^{40}_{\Lambda}$Ca	346.91	20.03 (18.7±1.1)	11.24 (11.0±0.6)	3.436	3.286	3.343	3.258	2.612
${}^{51}_{\Lambda}$V	456.05	22.10 (19.97±0.13)	13.88 (11.28±0.6)	3.547	3.490	3.461	3.540	2.735
${}^{89}_{\Lambda}$Y	790.09	24.19 (23.1±0.5)	17.78 (16.0±1.0)	4.216	4.204	4.145	4.270	3.130
${}^{139}_{\Lambda}$La	1186.67	25.18 (24.5±1.2)	20.49 (20.1±0.4)	4.835	4.895	4.776	4.991	3.657
${}^{208}_{\Lambda}$Pb	1659.77	26.58 (26.3±0.8)	22.67 (21.3±0.7)	5.490	5.602	5.439	5.718	4.017

A. Strategy to fit g_ρ and g_δ:

The NL3* parametrization used in RMF is fitted phenomenologically. All the masses and their coupling constants are adjusted to reproduce some specific experimental data. Therefore, it is not just to add one more parameter like g_δ, to study it's effect keeping all other parameters of NL3* as fixed. It might be possible that the physics described by g_δ may already be inbuilt in the sub parameters of NL3* and the inclusion of $\delta-$meson coupling may lead towards a double counting.

In this regard, we might expect a connection between g_δ and g_ρ since both the coupling constants are isospin dependent. In such a situation, there are two possible ways for this problem to avoid the double counting: (i) to consider a dependency on both g_δ and g_ρ couplings. In this case, modify the parameter g_ρ to fit an experimental data which is linked to both g_ρ and g_δ for each new given value of g_δ, such as binding energy or (ii) to get a completely new parameter set including this interaction to consider as a new degree of freedom from the beginning, i.e., start from an *ab initio* calculations as done in Ref. [54].

Here, we are not interested to make a new parameter by inclusion of this interaction but our motive is just to extract the contribution of $\delta-$meson in hypernuclei and corresponding normal nuclei. For this, we adopt the first approach to analyze the effect of g_δ on hypernuclei. The combination of g_δ and g_ρ are chose in such a way that for a given value of g_δ, the combined contribution of g_δ and g_ρ (by adjusting g_ρ) reproduces the physical observable which exactly match with the original predictions when g_δ was not included. We implement this scheme on binding energy which is the best physical observables to see every effects in the nuclear system. So, we choose the binding energies of ${}^{48}_{\Lambda}$Ca, ${}^{90}_{\Lambda}$Zr, ${}^{208}_{\Lambda}$Pb hypernuclei and corresponding their normal nuclei to consider as an experimental data. By inclusion of g_δ, the binding energies change from their original predictions. To bring back the NL3* binding energies for considered nuclei and hypernuclei, we modifiy the g_ρ coupling. In this way, we get various combinations of (g_ρ, g_δ) for different given values of g_δ. As we have already mentioned, the combinations of g_δ and g_ρ are possible because of both of the coupling constants are linked with isospin.

B. Binding energy, radii and single particle energy

Before going to task on $\delta-$meson, it is necessary to check the reliability of the parameter which is going to be used. For this purpose, we calculate the total binding energy (BE), single lambda binding energy (B_Λ) and radii for some selected hypernuclei whose experimental data are available. After analyzing Table I, we found that the lambda binding energy B_Λ (for s- and p-state) are quite comparable with the experimental data. For example, the B_Λ of ${}^{16}_{\Lambda}$N is 13.8 MeV in our calculation, and the experimental value is (13.76±0.16) MeV. It is obvious that the Λ hyperon exhibits its strange behaviour and enhance the binding of nucleons in hypernucleus. The other thing is, with increasing the mass number the lambda density becomes smaller in respect to nucleon density and as a result lambda radius (r_Λ) grows up. This observation is reflected in Table I, where r_Λ increases with increasing the nuclear number.

In this section, we analyze the effects of $\delta-$meson on considered hypernuclei and make their comparison with normal nuclei to demonstrate the affects, which is the central theme of the paper. For the same, we calculate the binding energy (BE), root mean square neutron (r_n), proton (r_p), charge (r_{ch}) and matter radius (r_t), and energy of first and last filled orbitals of ${}^{48}_{\Lambda}$Ca, ${}^{90}_{\Lambda}$Zr, ${}^{208}_{\Lambda}$Pb and ^{48}Ca, ^{90}Zr, ^{208}Pb with various combinations of g_ρ and g_δ.

In Fig. 1 (a) and (c), we have shown the binding energy difference ΔBE of ^{48}Ca and ${}^{48}_{\Lambda}$Ca between the two solutions obtained with (g_ρ, g_δ=0) and (g_ρ, g_δ), i.e.

$$\Delta BE = BE(g_\rho, g_\delta = 0) - BE(g_\rho, g_\delta), \qquad (15)$$

here $BE(g_\rho, g_\delta = 0)$ is the binding energy at $g_\delta = 0$ in the

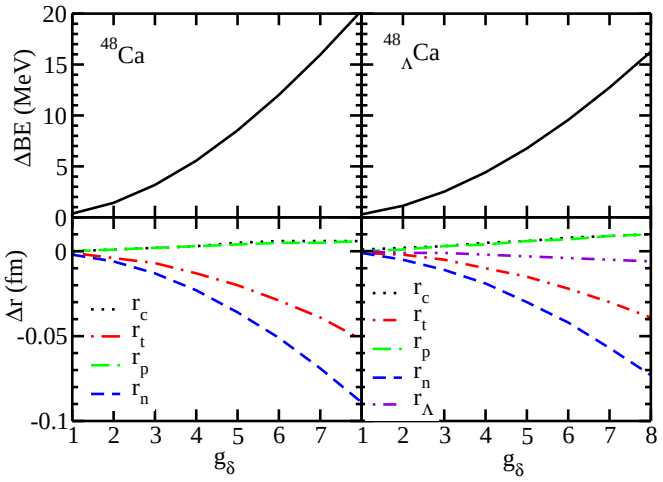

FIG. 1: (Color online) Binding energy (BE) and root mean square radius for ^{48}Ca and $^{48}_{\Lambda}$Ca using various combination of g_ρ and g_δ.

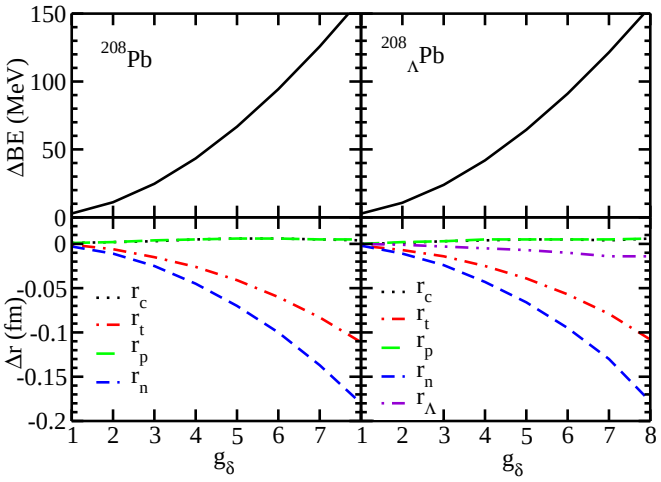

FIG. 3: (Color online) same as Fig.1 but for ^{208}Pb and $^{208}_{\Lambda}$Pb.

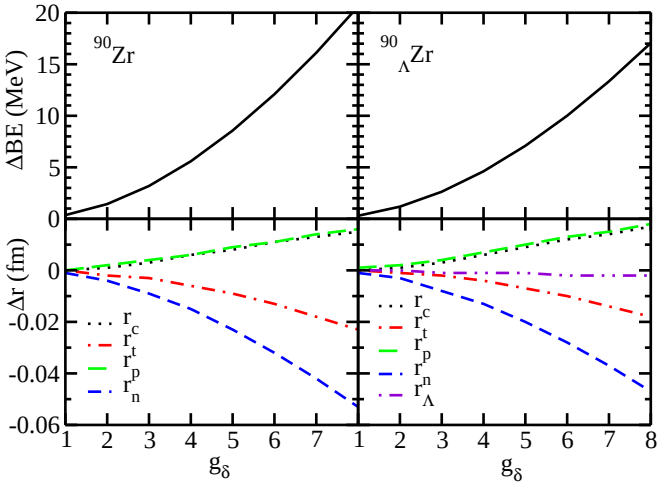

FIG. 2: (Color online) same as Fig.1 but for ^{90}Zr and $^{90}_{\Lambda}$Zr.

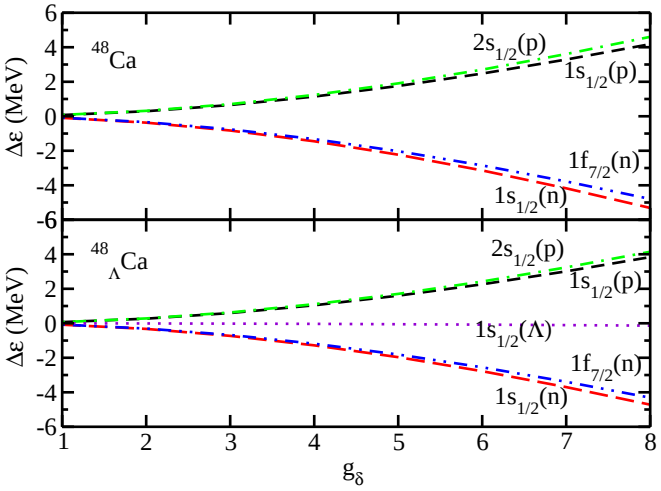

FIG. 4: (Color online) First ($1s^{n,p}$) and last ($1f^n$, $2s^p$) occupied orbits for ^{48}Ca and $^{48}_{\Lambda}$Ca using various (g_ρ, g_δ) combinations.

adjusted combination of (g_ρ, g_δ) and $BE(g_\rho, g_\delta)$ is the binding energy with non-zero value of g_δ in the adjusted combination which reproduce the same binding as pure NL3*. Here, the value of g_ρ used in adjusted combination with g_δ is different from the actual value given in original NL3* parameter set. In other words, we can say that, this strategy evolve a new parameter set with extra coupling constant g_δ, which also reproduces exactly same physical observables as NL3* set. Using this procedure, the contribution of $\delta-$ meson in binding energy is obtained from ΔBE. Similarly, the effect of $\delta-$meson in radius for both nuclei and hypernuclei can be seen from:

$$\Delta r = r(g_\rho, g_\delta = 0) - r(g_\rho, g_\delta), \tag{16}$$

where $r(g_\rho, g_\delta = 0)$ is the radius at $g_\delta = 0$ in the adjusted combination of (g_ρ, g_δ) and $r(g_\rho, g_\delta)$ is the radius in adjusted combination of g_ρ and g_δ with non zero value of g_δ, produces exactly same experimental value as pure NL3*. The magnitude of Δr with respect to g_δ for ^{48}Ca, ^{90}Zr, ^{208}Pb and their hypernucleus $^{48}_{\Lambda}$Ca, $^{90}_{\Lambda}$Zr, $^{208}_{\Lambda}$Pb are shown in Figs. 1−3. The same procedure has adopted to estimate the contribution of $\delta-$meson on single particle energy for considered hypernuclei and their non-strange counter parts, which are shown in Figures. 4−6. The difference in single particle energy ($\Delta\epsilon$) for a particular level is expressed as

$$\Delta\epsilon = \epsilon(g_\rho, g_\delta = 0) - \epsilon(g_\rho, g_\delta), \tag{17}$$

where $\epsilon(g_\rho, g_\delta = 0)$ is the single-particle energy for adjusted combination (g_ρ, g_δ) with $g_\delta = 0$, and $\epsilon(g_\rho, g_\delta)$ is energy of the occupied level with non zero value of g_δ.

From Figs.1−6, it is evident that the binding energies, radii, single particle energies and spin-orbit splitting of nuclei and

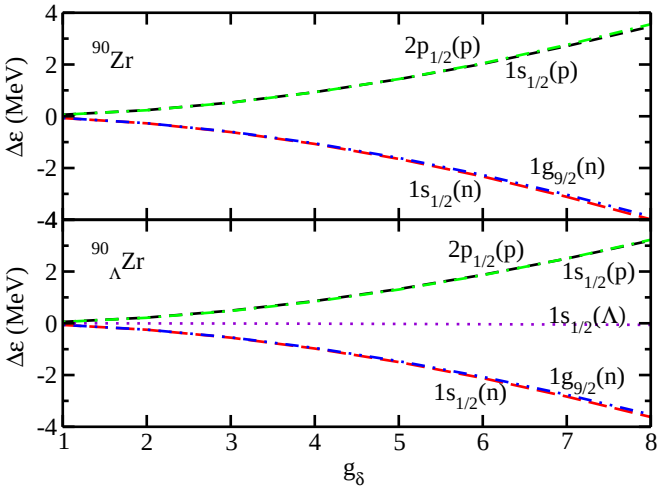

FIG. 5: (Color online) First ($1s^{n,p}$) and last ($1g^n$, $2p^p$) occupied orbits for ^{90}Zr and $^{90}_{\Lambda}$Zr using various (g_ρ, g_δ) combinations.

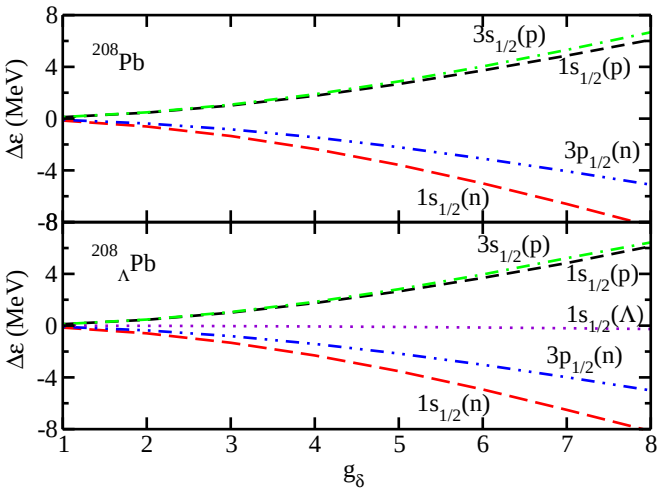

FIG. 6: (Color online) First ($1s^{n,p}$) and last ($3p^n$, $3s^p$) occupied orbits for ^{208}Pb and $^{208}_{\Lambda}$Pb using various (g_ρ, g_δ) combinations.

hypernuclei are affected with g_δ. Because of the presence of Λ hyperon, the contribution of $\delta-$meson in binding energies, radii and single particle energies are less in hypernuclei compared to normal nuclei. In other words, we can say that $\delta-$meson affects the physical observables less in strange nuclei relative to nonstrange nuclei. In contrary to this, the proton and charge radii are affected more in hypernuclei compared to normal nuclei. From the overview of g_δ on radii, we find that r_p and r_c are in opposite trend with r_n, r_t, and that's why the magnitude of differences of r_p and r_c increases with decreasing the asymmetry of the system by addition of hyperon. A very small reduction on lambda radius is observed with increasing strength of g_δ as shown in Figs. $1-$ 3, while the lambda potential is completely unaffected by g_δ. It may happen because of the rearrangement of the levels due to presence of lambda particle. It is to be noticed that there are no convergence solutions beyond $g_\delta \sim 8.0$.

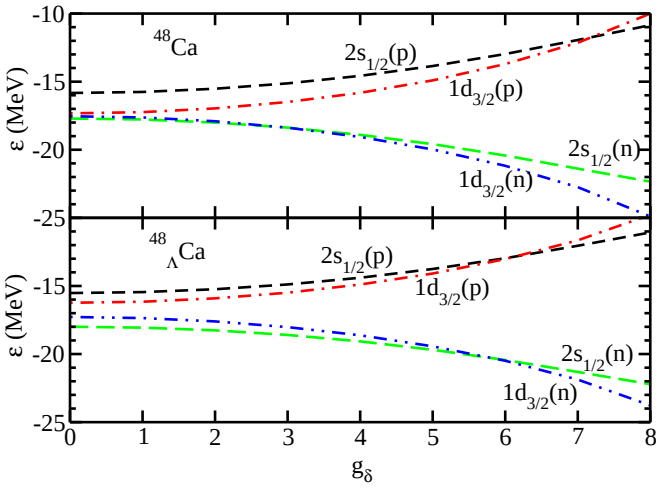

FIG. 7: (Color online) The effect of g_δ on spin-orbit splitting is observed for ^{48}Ca and $^{48}_{\Lambda}$Ca.

In Fig. 4, we have shown the change in single particle energy $\Delta\epsilon_{n,p}$ of the first ($1s^{n,p}$) and last ($1f^n$ and $2s^p$) occupied orbitals for ^{48}Ca, and $^{48}_{\Lambda}$Ca. In the same way, the change in first ($1s^{n,p}$) and last occupied levels ($1g^n$ and $2p^p$) for ^{90}Zr and $^{90}_{\Lambda}$Zr with the strength of g_δ is shown in Fig. 5. We also get the same trend in the magnitude of single particle energy difference for first ($1s^{n,p}$) and last occupied levels ($3p^n$ and $3s^p$) in $^{208}_{\Lambda}$Pb and corresponding their normal nucleus (^{208}Pb) which are displayed in Fig. 6. The magnitude of the difference of single particle energy for both neutron and proton (first and last occupied) orbitals of considered hypernuclei is small comparable to normal nuclei. Owing to zero isospin of Λ hyperon, the lambda orbit ($1s^{\Lambda}_{1/2}$) is unaffected with the strength of g_δ.

After analyzing the single particle spectra for both nuclei and hypernuclei, we notice that the orbitals make a shift with the strength of g_δ. In case of ^{48}Ca, the $2s^{n,p}_{1/2}$ levels are flipped with $1d^{n,p}_{3/2}$ in hypernucleus and normal nucleus also. It is shown in Fig. 8, the ^{90}Zr spectra pretend the flipping between $2p^p_{3/2}$ and $1f^p_{5/2}$ levels for both strange and nonstrange nuclei, however the strength is low, while the same orbitals ($2p^n_{3/2}$ and $1f^n_{5/2}$) for neutron goes apart from each other with increasing the strength of g_δ. The same trend as $^{48}_{\Lambda}$Ca is observed for $^{208}_{\Lambda}$Pb and its normal nucleus as shown in Fig 9. The proton level $1g^p_{9/2}$ close to flip with $2p^p_{1/2}$, and the neutron levels ($2d^n_{3/2}$ and $1h^n_{11/2}$) also show the flipping with a very little change in the value of single-particle energy $\Delta\epsilon$. In the analysis of neutron and proton single particle energy levels, we find that the trend of proton and neutron orbits are opposite to each other. This nature gives rise to effect of change in neutron and proton radius in opposite trend.

It is worthy to mention that the radius of ^{40}Ca is slightly more than that of ^{48}Ca (i.e. r_c=3.4776 of ^{40}Ca and r_c=3.4771

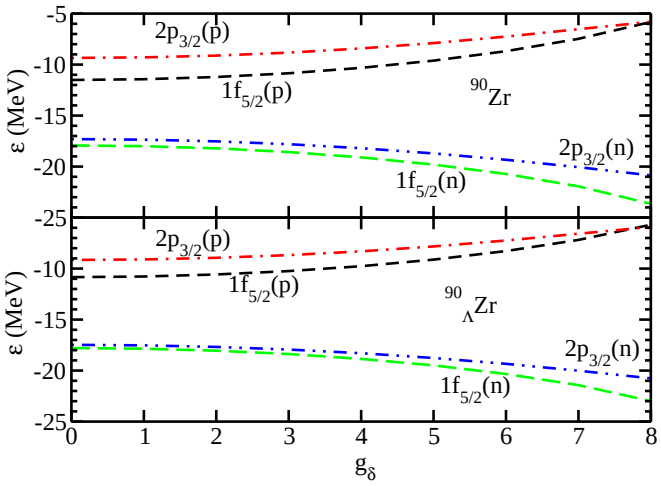

FIG. 8: (Color online) same as Fig.7 but for ^{90}Zr and $^{90}_{\Lambda}$Zr.

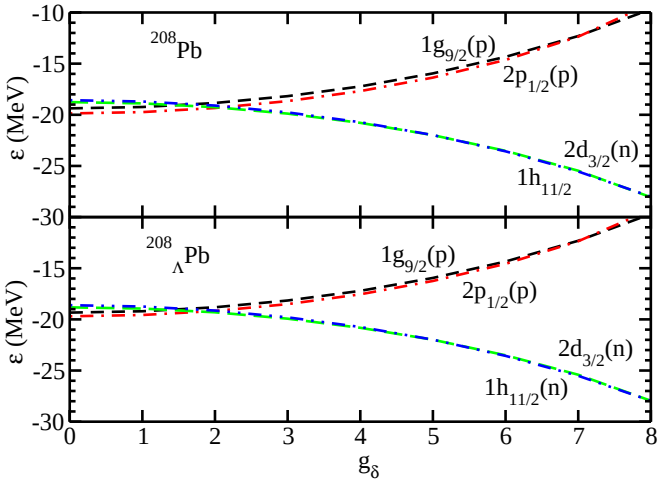

FIG. 9: (Color online) same as Fig.7 but for ^{208}Pb and $^{208}_{\Lambda}$Pb.

of ^{48}Ca [55, 56]), and this is difficult to explain by most of the nuclear models. We expact that similar anomaly may be occured in hyper-calcium ($^{40}_{\Lambda}$Ca and $^{48}_{\Lambda}$Ca) also and can be solved by the additional $\delta-$meson degree of freedom to the model. This mechanism can be used to solve the well known radius anomaly of ^{40}Ca and ^{48}Ca.

The neutron and lambda mean field potential for considered hypernuclei are plotted in Fig 10. The lambda central potential depth is found to be $V_\Lambda \sim 32.87, 30.41$ and 31.95 MeV for $^{48}_{\Lambda}$Ca, $^{90}_{\Lambda}$Zr and $^{208}_{\Lambda}$Pb, respectively. It is to be noticed that the amount of lambda potential is $38-40\%$ of nucleon potential. There are many of the calculations [51, 57, 58] in prediction of lambda potential depth and our results are consistent with these predictions. It is shown in Fig. 10 that both the potentials have similar shape but different depth. It is also found that the lambda potential is completely unaffected with the strength of $\delta-$meson coupling.

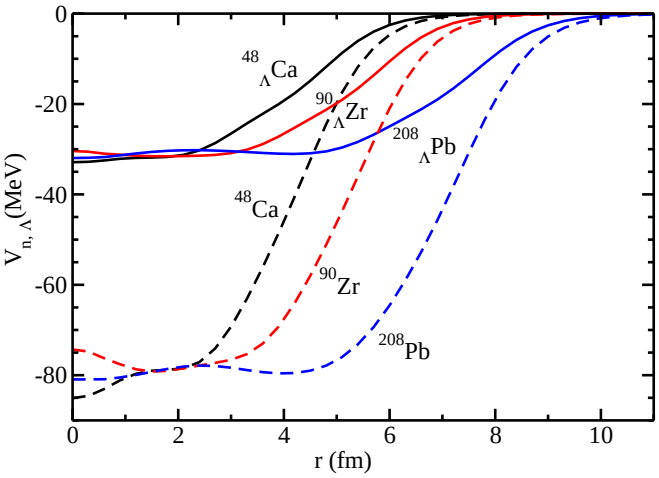

FIG. 10: (Color online) The neutron ($V_n = V_\sigma + V_\omega + V_\rho$) and lambda ($V_\Lambda = V_{\sigma\Lambda} + V_{\omega\Lambda}$) mean field potentials are plotted for $^{48}_{\Lambda}$Ca, $^{90}_{\Lambda}$Zr and $^{208}_{\Lambda}$Pb hypernuclei. The used parameter set is pure NL3*.

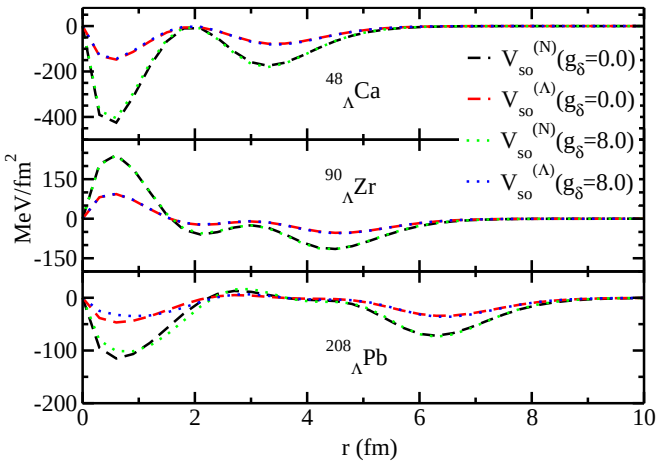

FIG. 11: (Color online) Radial dependence of spin-orbit potential (V^N_{so} and V^Λ_{so}) are plotted for $^{48}_{\Lambda}$Ca, $^{90}_{\Lambda}$Zr and $^{208}_{\Lambda}$Pb hypernuclei for different strength of g_δ.

C. Spin-orbit splitting

The spin-orbit interaction plays a crucial role in order to investigate the structural properties of normal as well as hypernuclei developed by the exchange of scalar and vector mesons [33, 59]. It is well known that the spin-orbit force in hypernuclei is weaker than normal nuclear system [33, 51, 60]. Here, we study the spin-orbit potential for nucleon (V^N_{so}) and hyperon (V^Λ_{so}) in hypernuclei and also analyze the effect of g_δ on spin-orbit interaction. The spin-orbit potentials are displayed in Fig. 11 for considered hypernuclei. To see the effect of g_δ, we make a plot with g_δ=0.0 and for g_δ=8.0, which is the largest allowed strength of delta-meson coupling. Figure 11

reveals that the spin-orbit potential for hyperons is weaker than their normal counter parts and these results are consistent with existing predictions [33, 51, 60]. It is clearly seen from the Fig. 11 that the delta-meson coupling does not have any valuable impact on spin-orbit interaction. Actually, no change in spin-orbit potential is observed for ${}^{48}_{\Lambda}$Ca and ${}^{90}_{\Lambda}$Zr hypernuclei. Rather than this, the spin-orbit potentials in ${}^{208}_{\Lambda}$Pb hypernucleus is affected by a very little amount. This trend reflects that the measurable effect of g_δ on spin-orbit interaction can be observed from a system with large isospin asymmetry for example, heavy or superheavy nuclei and hypernuclei.

IV. SUMMARY AND CONCLUSIONS

In summary, we study the contribution as well as importance of $\delta-$meson coupling in non-linear RMF model for hypernuclei. The lambda potential depth is found to be consistent with other predictions [51, 57, 58]. The calculated B_Λ for considered nuclei are quite agreeable with the experimental data. In the present calculation, we have included it to reveal the effects of g_δ coupling strength on hypernuclei which are found to be significant. It is clear to say that g_δ affects every piece of physical observables of hypernuclei, like binding energy, radii, single particle energy and spin-orbit splitting for nuclear system with N$\neq$Z, but the magnitude of affects is less comparable to normal nuclei. Contrary to this, the proton and charge radii are affected relatively more than normal nuclear case. A very small reduction in lambda radius is also observed with increasing strength of $\delta-$meson coupling. However, the lambda potential is completely unaffected by $\delta-$meson coupling strength due to zero isospin nature of Λ particle. The variation of spin-orbit interaction is discussed in respect of δ-meson coupling. This coupling does not have any significant impact on spin-orbit potential for considered hypernuclei but reflects that its impact would be measurable for a system with large isospin asymmetry. It is clearly seen that the contribution of $\delta-$meson is more effective with the magnitude of asymmetry of the system. From the given results, it is concluded that $\delta-$meson has indispensable contribution not only in asymmetric nuclei but also for hypernuclei.

The $\delta-$meson coupling may prove to be a significant degree of freedom for resolving the charge radius anomaly which is appeared in ^{40}Ca and ^{48}Ca and also if happened in corresponding hypernuclei. The production of ${}^{48}_{\Lambda}$Ca hypernucleus is possible in future due to advanced experimental facilities across the world.

ACKNOWLEDGMENTS

One of the author (MI) would like to acknowledge the hospitality provided by Institute of Physics, Bhubaneswar during the work.

[1] J. Cugnon, A. Lejeune and H. -J. Schulze, Phys. Rev. C **62**, 064308 (2000).
[2] B. F. Gibson and E. V. Hungerford III, Phys. Rep. **257**, 349 (1995).
[3] M. Rufa, J. Schaffner, J. Maruhn, H. Stöcker, W. Greiner and P. -G. Reinhard, Phys. Rev. C **42**, 2469 (1990).
[4] M. Rufa, H. Stöcker, P. -G. Reinhard, J. Maruhn and W. Greiner, J. Phys. G: Nucl. Phys. **13**, L143 (1987).
[5] E. Hiyama, T. Motoba, T. A. Rijken and Y. Yamamoto, Prog. Theor. Phys. Suppl., **185**, 1 (2010).
[6] E. Hiyama, M. Kamimura, Y. Yamamoto, T. Motoba and T. A. Rijken, Prog. Theor. Phys. Suppl., **185**, 106 (2010).
[7] H. -J. Schulze, Nucl. Phys. A **835**, 19 (2010).
[8] B. Povh, Prog. Part. Nucl. Phys. **18**, 183 (1987).
[9] R. Chrien and C. Dover, Ann. Rev. Nucl. Part. Sci. **39**, 113 (1989).
[10] A. Gal, Few. Body. Syst. **45**, 105 (2009).
[11] J. Schaffner, C. B. Dover, A. Gal, C. Greiner, D. J. Millener and H. Stöcker, Ann. Phys. (N.Y.) **235**, 35 (1994).
[12] A. Gal, Prog. Theor. Phys. Suppl., **186**, 270 (2010).
[13] A. Gal, Prog. Theor. Phys. Suppl., **156**, 1 (2004).
[14] E. Hiyama, Few. Body. Syst. **53**, 189 (2012).
[15] T. Harada, Nucl. Phys. A **754**, 86c (2005).
[16] D. E. Lanskoy, Phys. Rev. C **58**, 3351 (1998).
[17] H. Bando, T. Motoba and J. Zofka, Int. J. Mod. Phys. A **5**, 4021 (1990).
[18] Y. H. Tan, X. H. Zhong, C. H. Cai, P. Z. Ning, Phys. Rev. C **70**, 054306 (2004).
[19] B. Lu, E. Zhao and S. Zhou, Phys. Rev. C **84**, 014328 (2011).
[20] D. Vretenar, W. Pošchl, G. A. Lalazissis and P. Ring, Phys. Rev. C **57**, R1060 (1998).
[21] X. -R. Zhou, A. Polls, H. -J. Schulze and I. Vidaña, Phys. Rev. C **78**, 054306 (2008).
[22] O. Hashimoto and H. Tamura, Prog. Part. Nucl. Phys. **57**, 564 (2006).
[23] M. Rayet, Ann. Phys. (N.Y.) **102**, 226 (1976).
[24] M. Rayet, Nucl. Phys. A **367**, 381 (1981).
[25] N. Guleria, S. K. Dhiman and R. Shyam, Nucl. Phys. A **886**, 171 (2012).
[26] X. -R. Zhou, H. -J. Schulze, H. Sagawa, C. X. Wu and E. G. Zhao, Phys. Rev. C **76**, 034312 (2007).
[27] M. T. Win, K. Hagino and T. Koike, Phys. Rev. C **83**, 014301 (2011).
[28] N. K. Glendenning, D. Von-Eiff, M. Haft, H. Lenske and M. K. Weigel, Phys. Rev. C **48**, 889 (1993).
[29] J. Mares and B. K. Jennings, Phys. Rev. C **49**, 2472 (1994).
[30] R. Xu, C. Wu and Z. Ren, J. Phys. G: Nucl. Part. Phys. **39**, 085107 (2012).
[31] J. Mares and J. Zofka, Z. Phys. A **333**, 209 (1989).
[32] J. Mares and J. Zofka, Z. Phys. A **345**, 47 (1993).
[33] R. Brockmann and W. Weise, Phys. Lett. B **69**, 167 (1977).
[34] J. Boguta and S. Bohrmann, Phys. Lett. B **102**, 93 (1981).
[35] B. D. Serot and J. D. Walecka, Adv. Nucl. Phys. **16**, 1 (1986).
[36] B. D. Serot, Rep. Prog. Phys. **55**, 1855 (1992).
[37] W. Pannert, P. Ring and J. Boguta, Phys. Rev. Lett. **59**, 2420 (1981).
[38] P. Ring, Prog. Part. Nucl. Phys. **37**, 193 (1996).
[39] S. K. Patra and C. R. Praharaj, Phys. Rev. C **44**, 2552 (1991).
[40] S. K. Patra, R. K. Gupta, B. K. Sharma, P. D. Stevenson and W. Greiner, J. Phys. G: Nucl. Part. Phys. **34**, 2073 (2007).

[41] J. D. Walecka, Ann. Phys. (N.Y.) **83**, 491 (1974).
[42] J. Boguta and A. R. Bodmer, Nucl. Phys. A **292**, 413 (1977).
[43] L. I. Schiff, Phys. Rev. **84**, 1 (1951).
[44] S. Kubis and M. Kutschera, Phys. Lett. B **399**, 191 (1997).
[45] X. Roca-Maza, X. Viñas, M. Centelles, P. Ring and P. Schuck, Phys. Rev. C **84**, 054309 (2011).
[46] Shailesh K. Singh, S. K. Biswal, M. Bhuyan and S. K. Patra, *arXiv:1310.5689v1* (2013).
[47] Y. Sugahara and H. Toki, Prog. Theor. Phys. **92**, 803 (1994).
[48] M. T. Win and K. Hagino, Phys. Rev. C **78**, 054311 (2008).
[49] H. -F. Lü, J. Meng, S. Q. Zhang and S. G. Zhou, Eur. Phys. J. A **17**, 19 (2003).
[50] G. A. Lalazissis, S. Karatzikos, R. Fossion, D. Pena Arteaga, A. V. Afanasjev and P. Ring, Phys. Lett. B, **671**, 36 (2009).
[51] C. M. Keil, F. Hoffmann and H. Lenske, Phys. Rev. C **61**, 064309 (2000).
[52] H. Shen, F. Yang and H. Toki, Prog. Theor. Phys. **115**, 325 (2006).
[53] Q. N. Usmani and A. R. Bodmer, Phys. Rev. C **60**, 055215 (1991).
[54] F. Hofmann, C. M. Keil and H. Lenske, Phys. Rev. C **64**, 034314 (2001).
[55] I. Angeli and K. P. Marinova, At. data and Nucl. data tables **99**, 69 (2013).
[56] S. Haddad, Chin. J. Phys. **50**, 392 (2012).
[57] T. Motoba, H. Bando, R. Wünsch and J. Zofka, Phys. Rev. C **38**, 1322 (1988).
[58] D. H. Davis, R. L. Setti, M. Raymund, O. Skjeggestad, G. Tomasini, J. Lemonne, P. Renard and J. Sacton, Phys. Rev. Lett. **9**, 464 (1962).
[59] W. Koepf and P. Ring, Z. Phys. A **339**, 81 (1991).
[60] S. Ajimura et. al., Phys. Rev. Lett. **86**, (2001).